Tau protein quantification in skin biopsies differentiates tauopathies from alpha-synucleinopathies

Elena Vacchi,[1,2] Edoardo Lazzarini,[3] Sandra Pinton,[1] Giacomo Chiaro,[1,4] Giulio Disanto,[4] Francesco Marchi,[5] Thomas Robert,[2,5] Claudio Staedler,[4] Salvatore Galati,[2,4] Claudio Gobbi,[2,4] Lucio Barile,[2,3,6] Alain Kaelin-Lang[1,2,4,7] and Giorgia Melli[1,2,4]

1. 1 Laboratory for Biomedical Neurosciences, Neurocenter of Southern Switzerland, Ente Ospedaliero Cantonale, Lugano, Switzerland

2. 2 Faculty of Biomedical Sciences, Università della Svizzera italiana, Lugano, Switzerland

3. 3 Laboratory for Cardiovascular Theranostics, Cardiocentro Ticino Institute, Ente Ospedaliero Cantonale, Lugano, Switzerland

4. 4 Neurology Department, Neurocenter of Southern Switzerland, Ente Ospedaliero Cantonale, Lugano, Switzerland

5. 5 Neurosurgery Department, Neurocenter of Southern Switzerland, Ente Ospedaliero Cantonale, Lugano, Switzerland

6. 6 Institute of Life Science, Scuola Superiore Sant'Anna, Pisa, Italy

7. 7 Department of Neurology, Inselspital, Bern University Hospital, University of Bern, Bern, Switzerland

Correspondence to: PD Dr Med Giorgia Melli

Laboratory for Biomedical Neurosciences, Neurocenter of Southern Switzerland, Ente Ospedaliero Cantonale, via Francesco Chiesa 5, 6500 Bellinzona, Switzerland

E-mail: giorgia.melli@eoc.ch

Running title: Tau protein in skin biopsy

Abstract

Abnormal accumulation of microtubule-associated protein tau (τ) is a characteristic feature of atypical parkinsonisms with tauopathies such as Progressive Supranuclear Palsy (PSP) and Corticobasal Degeneration (CBD). However, pathological τ has also been observed in α-synucleinopathies like Parkinson's Disease (PD) and Multiple System Atrophy (MSA). Based on the involvement of peripheral nervous system in several neurodegenerative diseases, we characterized and compared τ expression in skin biopsies of patients clinically diagnosed with PD, MSA, PSP, CBD, and in healthy control subjects.

In all groups, τ protein was detected along both somatosensory and autonomic nerve fibers in the epidermis and dermis by immunofluorescence. We found by western blot the presence of mainly two different bands at 55 and 70 KDa, co-migrating with 0N4R/1N3R and 2N4R isoforms, respectively. At the RNA level, the main transcript variants were 2N and 4R, and both resulted more expressed in PSP/CBD by real-time PCR. ELISA assay demonstrated significantly higher levels of total τ protein in skin lysates of PSP/CBD compared to the other groups. Multivariate regression analysis and ROC curves analysis of τ amount at both sites showed a clinical association with tauopathies diagnosis and high diagnostic value for PSP/CBD *vs*. PD (sensitivity 90%, specificity 69%) and PSP/CBD *vs*. MSA (sensitivity 90%, specificity 86%). τ protein increase correlated with cognitive impairment in PSP/CBD.

This study is a comprehensive characterization of τ in the human cutaneous peripheral nervous system in physiologic and pathologic conditions. The differential expression of τ, both at transcript and protein levels, suggests that skin biopsy, an easily accessible and minimally invasive exam, can help in discriminating among different neurodegenerative diseases.

Keywords: tau protein; skin biopsy; Parkinson's disease; tauopathies; biomarkers.

Abbreviations: AUC = Area under the curve; BDI-II = Beck Depression Inventory-II; βTubIII = Beta Tubulin III; COMPASS-31 = Composite Autonomic Symptom Score 31; CI = Confidence intervals; CBD = Corticobasal degeneration; HC = Healthy control; H&Y = Hoehn and Yahr Scale; IF = Immunofluorescence; IENFD = Intraepidermal nerve fiber density; LEDD = Levodopa equivalent daily dose; LDA = Linear Discriminant Analysis; MMSE = Mini-Mental State Examination; MoCA = Montreal Cognitive Assessment; MDS-UPDRS = Movement Disorder Society Unified Parkinson's Disease Rating Scale; MSA = Multiple system atrophy; MAP = Muscle arrector pili; OR = Odds ratios; o.n. = Over night; PD = Parkinson's disease; PCR = Polymerase Chain Reaction; PSP = Progressive supranuclear palsy; PGP9.5 = Protein gene product 9.5; ROC = Receiver operating characteristics; RBD = REM sleep Behavior Disorder; RT = Room Temperature; SbG = Sebaceous Gland; SG = Sweat glands; τ = Tau protein; Wb = Western Blot.

Introduction

Tau (τ) is a microtubule-associated protein coded by *MAPT* gene[1]. In the adult human central nervous system, post-transcriptional modifications of τ pre-mRNA can produce six different mature mRNA molecules: 0N3R, 0N4R, 1N3R, 1N4R, 2N3R, 2N4R[1]. Such isoforms result from the combination of alternative splicing of exons 2 and 3, generating the amino-terminal inserts 0N, 1N, and 2N, and alternative splicing of exon 10 coding for three or four carboxy-terminal repeat domains named respectively 3R and 4R[1]. τ is also subjected to several post-translational modifications[2,3], such as phosphorylation[4], acetylation[5], and ubiquitination[6], which strongly regulate its function. Mutations in the *MAPT* gene or abnormalities in post-translational regulatory mechanisms can induce τ aggregations and toxicity; for instance, hyper-phosphorylation in different sites of τ seems to precede and enhance aggregation[7-9]. Although the presence of mutated and/or aggregated τ in the brain is the hallmark of a family of neurodegenerative diseases called tauopathies[10], such as Alzheimer's disease, Progressive Supranuclear Palsy (PSP), and Corticobasal Degeneration (CBD), pathological τ has also been observed in synucleinopathies at later stages like Parkinson Disease (PD)[11] and multiple system atrophy (MSA)[12,13].

Previous studies have demonstrated the presence of hyper-phosphorylated τ in tauopathies patients' peripheral tissues like olfactory[14] and oral[15] epithelium and colon specimens[16], boosting the possibility to use peripheral tissues not only for research but also as a diagnostic tool. Due to its easy, minimally-invasive accessibility and its great content in nerve fibers, skin is a candidate for biomarkers discovery in neurodegenerative disorders[17]. Indeed, skin biopsy has already been exploited to detect α-Synuclein, the pathological hallmark of PD, in patients with synucleinopathies[18-20] and to demonstrate and quantify a small fiber neuropathy in PD by intraepidermal nerve fiber density (IENFD) measurement[20-22].

Nevertheless, few studies have explored the expression of τ in peripheral tissues and skin[23-26]; in particular, a comprehensive investigation of τ in human skin in physiological and pathologic conditions is lacking. Thus, the aims of this study were to: 1) assess the presence of total and phosphorylated forms of τ in skin biopsy from HC and patients clinically diagnosed with PD, MSA, and PSP/CBD; 2) quantitatively analyze differences in τ expression among groups; 3) evaluate the diagnostic capacity of cutaneous τ for PD, MSA, and PSP/CBD.

Materials and methods

Subjects' recruitment

Patients were consecutively recruited from the movement disorders outpatient clinic at NSI Lugano from July 2015 to October 2021. HC were recruited among hospital staff and patients' partners as part of the NSIPD001 study[20].

Inclusion criteria for PD were: a definite clinical diagnosis according to the UK Brain Bank diagnostic criteria[27], no family history, and no significant cognitive impairment or dysautonomic symptoms in the history. The inclusion criteria for MSA[28], PSP[29], and CBD [30] were based on published diagnostic criteria. Exclusion criteria were significant comorbidities diabetes, renal failure, thyroid pathology, vitamin B12 deficiency, HIV infection, syphilis, coagulopathy, acute and chronic inflammatory diseases, and chemotherapy.

This study was performed in line with the principles of the Declaration of Helsinki. Subjects were included according to the study protocol, approved by the Cantonal Ethics Committee. All enrolled subjects gave written informed consent to the study.

Clinical assessments

PD, MSA, PSP, and CBD patients underwent a standard clinical evaluation: disease gravity was assessed by Hoehn and Yahr scale (H&Y)[31] and the Movement Disorder Society-Unified Parkinson's Disease Rating Scale[32] (scale I - clinical evaluation of mental state, behaviour, and mood; scale II - self-assessment by the patient of specific daily activities; scale III - clinical evaluation of motor skills); cognitive profile by Mini-Mental State Evaluation (MMSE)[33] and Montreal Cognitive Assessment (MoCA)[34] scales; mood disorder by Beck Depression Inventory-II (BDI-II) scale[35]; autonomic dysfunction by Composite Autonomic Symptom Score 31 (COMPASS-31, OH: orthostatic hypotension, VM: vasomotor, SM: sudomotor, GI: gastrointestinal, BL: bladder, PM: pupillomotor)[36]; Rapid eye movement sleep Behavior Disorder (RBD) by RBD screening questionnaire[37]; olfactory function by Sniffin' Sticks Smell test (Burghart Messtechnik GmbH, Wedel, Germany). Levodopa equivalent daily dose (LEDD) was calculated[38].

Skin biopsy

On the more clinically affected side, a double three mm-diameter punch skin biopsy was performed in the neck at C8 dermatomal level (cervical) and in the distal leg 10 cm above lateral malleolus (ankle)[20,39]. For each anatomical site, one biopsy was fixed for immunofluorescence (IF) studies[20,22,39], and one biopsy was stored at -80° until further analysis by Western blot (Wb), ELISA, or Polymerase Chain Reaction (PCR) assays.

Immunofluorescence

IF assays were performed as previously described[20,22,39]. Briefly, skin biopsies were fixed overnight (o.n.) at 4°C in Paraformaldehyde-Lysine-Periodate 2% fixative. The day after, they were frozen and cut with a cryotome to obtain 50 µm-thin tissue sections for free-floating immunofluorescence analysis. Three non-consecutive sections per biopsy were incubated o.n. at room temperature (RT) with a panel of primary antibodies (Table 1). The day after, sections were washed twice in tris-buffered saline (TBS; ThermoFisher Scientific, Waltham USA) for 10 minutes at RT and incubated with the appropriate fluorescence-tagged secondary antibody (Table 1) for 90 minutes at RT. Cell nuclei were counterstained with 4′,6-diamidino-2-phenylindole (DAPI, Sigma-Aldric h, Saint Louis USA, 1:5000). Sections were viewed and analyzed with a Nikon confocal microscope (40x magnification, successive frames of 2µm increments on a Z-stack plan) using NIS Elements 4.11.01 imaging software.

Intraepidermal nerve fiber density

Intraepidermal nerve fiber density (IENFD) was assessed as a measure of small fiber neuropathy[40-43]. At least three tissue sections per localization per patient were stained with the primary antibody against Protein Gene product 9.5 (PGP9.5, Abcam, Cambridge UK, 1:1000). PGP9.5 positive nerve fibers crossing the dermal-epidermal junction were counted. The length of the section was measured using NIS Elements 4.11.01 imaging software (Tool: manual measure). IENFD was obtained by dividing the number of fibers by the length of the section and expressed as the "number of fibers/mm". IENFD was determined at both ankle and cervical sites, and total IENFD was calculated as the mean of nerve densities at both localizations[22].

Western blot

Skin biopsies from HC (*n*=20), PD (*n*=26), MSA (*n*=9), and PSP/CBD (*n*=10) were homogenized in 1mL of radioimmunoprecipitation assay buffer (RIPA; Sigma Aldrich, Saint Louis, USA) supplied with protease inhibitor (Sigma Aldrich, Saint Louis, USA, 1:10) and used for Wb and ELISA assays. After centrifugation at 13000 rpm for 3 minutes, supernatants were analyzed. Protein quantification was determined with the QuantiPro BCA assay kit (Sigma Aldrich, Saint Louis, USA). Proteins were separated on SDS-PAGE 12% acrylamide gel and transferred onto PVDF membranes, which were subsequently incubated with a panel of primary antibodies (Table 1) o.n. at 4°C. After three washing in TBS-Tween 0.1% incubation with secondary antibody for 90 minutes was performed at RT (Table 1). The membranes were analyzed with the Odyssey CLx system (Li-cor Biosciences, Lincoln, Nebraska). Phosphorylated τ quantification in skin extracts was performed by an expert, blind to the clinical diagnosis, with IS Image studio software Ver 5.0. The intensity of the two bands at 70kDa and 55kDa was normalized to the β-actin signal. The sum of the two bands was calculated for each patient and each localization.

ELISA

Homogenized samples were diluted at 1:20 in PBS 1x (ThermoFisher Scientific, Waltham, USA). 50 µL of diluted sample per well were put in a coated 96 well-plate (Nunc MaxiSorp, ThermoFisher Scientific, Waltham, USA), o.n at 4°C. Subsequently, samples were washed three times with PBS-Tween 0.05% and then incubated with: blocking buffer (PBS-Tween 0.05%, Bovine Serum Albumin 1%) for 1h at 37°C; primary antibody (unphosphorylated and phosphorylated at Ser262 human Tau, 1:500; Table 1) for 1h at 37°C; secondary antibody (Goat anti-Rabbit HRP, Biorad, Hercules USA, 1.5000) for 1h at 37°C. 50 µL of TMB-Substrate (ThermoFisher Scientific, Waltham USA) were added to each well, and absorbance (450nm) was measured immediately after adding the stop solution (Phosphoric Acid 2M) by Infinite M-PLEX TECAN instrument (Männedorf, Switzerland). τ concentration was normalized to the sample protein concentration (QuantiPro BCA assay kit).

RNA extraction and reverse transcription

Skin biopsies from HC (*n*=4), PD (*n*=5), MSA (*n*=5), PSP (*n*=4)/CBD (*n*=1) were homogenized in 1mL of TRIzol (ThermoFisher Scientific, Waltham USA). A smaller cohort was analyzed based on the tissue availability in the bio-bank of the NSIPD001 study (demographic and clinical characteristics are summarized in Supplementary Table 1). As a positive control for PCR assays, we analyzed a little cortical sample from a patient without a neurodegenerative disorder who underwent a craniotomy for diagnostic purposes after obtaining informed consent. 250µL of chloroform (Sigma Aldrich, Saint Louis, USA) was added to the homogenate, which was subsequently centrifuged at 10.000 rpm for 5 minutes. The aqueous phase was transferred to a new sterile tube containing 550µL of isopropanol (Sigma Aldrich, Saint Louis, USA). Samples were kept at RT for 5 minutes, followed by 1hour at -80°. Next, samples were centrifuged at 14.000 rpm for 20 minutes; the supernatant was discharged and substituted with 500µL of 75% ethanol (Sigma Aldrich, Saint Louis, USA). Ethanol was removed after centrifugation at 9.500 rpm for 5 minutes, and pellets were resuspended in 20µL of pure water. The total RNA quantification of samples was determined by Nanodrop 200 Spectrophotometer (ThermoFisher Scientific, Waltham, USA). 800ng of total RNA were reverse transcribed into cDNA with GoScript™ Reverse Transcription System (Promega Corporation, Madison USA), following the manufacturer's protocol. The resulting cDNA was stored at − 20 °C until use.

PCR assay

PCR was performed using the Dream-Taq DNA polymerase (ThermoFisher Scientific, Waltham USA) following manufacturer protocol, the annealing temperature was set at 60°, and 35 reaction cycles were performed. To examine the alternate splicing of exons 2 and 3 at the N-terminal domain of τ, the cDNA was amplified using the primers for exon 1 (F 5'-ACACGGACGCTGGCCTGAAA-3') and exon 4 (R 5'-TCACGTGACCAGCAGCTTCGTCTT-3'). To evaluate the splicing of exon 10 in the microtubule-binding domain repeat region, the cDNA was amplified using the primers for exon 9 (F 5'-CAGTGGTCCGTACTCCACCCAA-3') and exon 11 (R 5'-TGGTTTATGATGGATGTTGCCTAATGAG-3'). *GAPDH* gene was used as a housekeeper and amplified with the primers: F 5'- TGCACCACCAACTGCTTAGC-3' and R 5'-

GGCATGGACTGTGGTCATGAG-3'. Primers were designed with the primer design tool PrimerBlast (NCBI).

The resulting PCR products were separated by 2,5% Tris-acetate-EDTA agarose gel electrophoresis. Obtainable bands were 2N amplicon of 255 base pairs (bp), 1N and 0N of respectively 168bp, and 81bp length, 4R and 3R of respectively 317bp and 224bp. *GAPDH* amplicon was 87 bp.

Real-time PCR

Real-time PCR was performed using SsoAdvanced Universal SYBR Green Supermix (Biorad, Hercules USA), following the manufacturer's instructions in triplicate. *MAPT* gene was amplified with two different pairs of primers published on Primerbank: F 5'-CCAAGTGTGGCTCATTAGGCA-3', R 5'-CCAATCTTCGACTGGACTCTGT-3', and F 5'-GAGTCCAGTCGAAGATTGGGT-3', R 5'-GGCGAGTCTACCATGTCGATG-3'.

The 2N splicing variants of the *MAPT* gene were amplified using the primers for exon 3 (F 5'-TGACAGCACCCTTAGTGGATGA-3') and exon 4 (R 5'-TCACGTGACCAGCAGCTTCGTCTT-3'); while the 4R splicing variants were amplified using the primers for exon 9 (F 5'-CAGTGGTCCGTACTCCACCCAA-3') and a primer spanning the exon 9 and 10 (R 5'-AGCTTCTTATTAATTATCTGCACCTTC-3'). Primers were designed with PrimerBlast tool (NCBI). *RPL27* gene was amplified as endogenous controls for normalization (F 5'-TGGTAGGGCCGGGTGGTTGC-3'; R 5'-ACTTTGCGGGGTAGCGGTC-3'). The PCR reaction was carried out on CFX-Connect real-time PCR Detection System (Biorad, Hercules USA): τ cDNA expression was calculated by $\Delta\Delta$Ct methods as previously reported[44]. The real-time PCR was performed in triplicate, pooling together samples of subjects of the same group. Sample pools were obtained by loading the same amount of cDNA from every sample, and the same quantity of cDNA pools per group was loaded for real-time PCR amplification. Values were normalized to the mean of τ cDNA expression of HC at the ankle and cervical sites.

Statistical Analysis

Statistical analysis was performed using IBM SPSS Statistics 26.0. The distribution of variables was assessed by the Kolmogorov-Smirnov test. 1-way ANOVA test with post-hoc Bonferroni's test for multiple comparisons was used for normally distributed variables (age), expressed as mean ± standard deviation. Kruskal-Wallis test was used for non-normally distributed variables (disease duration, H&Y, MDS-UPDRS, BDI-II, MMSE, MoCA, COMPASS-31, Olfactory test, RBD, LEDD, Tau concentration, IENFD), expressed as medians and interquartile range. χ^2 or Fisher's exact tests were used for categorical variables (sex), defined as a percentage (%). Univariate and multivariate logistic regression was used to test compound τ for association with disease status (PSP/CBD *vs*. all other groups and PSP/CBD *vs*. MSA/PD), with odds ratio and 95%CI intervals calculation. Receiver operating characteristics (ROC) curves analysis was used to evaluate the area under the curve (AUC) and compare selected variables' diagnostic performances. Younden index (J = Sensitivity + Specificity -1) was calculated to determine the cut-off with greater accuracy. For Linear Discriminant Analysis (LDA), canonical components 1 and 2 were calculated from weighted linear combinations of variables to maximize separation between the four groups (HC, PD, MSA, PSP/CBD); in the plot, each patient is represented by a point, the centroid indicates the mean of (canonical 1 and canonical 2) for each diagnosis. Correlations were evaluated by Pearson's R test and regression curve analysis; correlations were considered strong for R between |1.0| and |0.5|, moderate between |0.5| and |0.3|, weak between |0.3 and |0.1|. A *P*-value lower than 0.05 was considered significant.

Data availability

The raw data that support the findings of this article are available on request to the corresponding author.

Results

Patients

Thirty-one patients with idiopathic PD, 14 with probable MSA, 15 PSP/CBD (11 probable PSP, 4 possible CBD), and 24 age-matched HC for the PD group were enrolled. The demographic

characteristics and clinical assessments of the study groups are summarized in Table 2. Sex ratio did not differ across all groups; while disease duration did not differ across patients; PSP/CBD subjects were significantly older than HC. MSA and PSP/CBD patients had a more severe disease burden than PD, as measured by H&Y and MDS-UPDRS scales, and a higher cognitive impairment as measured by MMSE. PSP/CBD subjects were more depressed than PD as measured by the BDI-II scale and showed a more severe cognitive impairment than both PD and MSA, as assessed by MoCA. Finally, MSA patients had greater autonomic impairment in genitourinary function than PD and PSP/CBD, as measured by the COMPASS-31 questionnaire (bladder [BL] subdomain). No significant difference in LEDD was detected among groups.

τ protein is expressed in epidermal and dermal nerve fibers

The presence of τ protein in skin biopsies of HC at both anatomical sites was assessed by IF assays with several primary Abs against different epitopes of τ (Table 1 and Fig. 1A): the N-terminal region (Tau13), the proline-rich domain (HT7 and Tau5), and the tubulin-binding region (Tau). They all showed clear immunoreactivity along cutaneous nerve fibers (Fig. 1B) counterstained with the panaxonal markers PGP 9.5 or Beta Tubulin class III (βTubIII). τ positive nerve fibers were found in the epidermis, dermis, and autonomic structures such as sweat glands (SG), sebaceous glands (SbG), and muscle arrector pili (MAP). Indeed, the colocalization of τ with a specific cholinergic marker (vasoactive intestine peptide, VIP) and adrenergic marker (tyrosine Hydroxylase, TH) confirmed the presence of τ in autonomic nerve fibers as well (Fig. 1C).

τ protein was detected in skin biopsies from ankle and cervical sites in PD, MSA, and PSP/CBD (Fig. 2). Overall, qualitative IF analysis showed high levels of τ in the PSP/CBD group, especially at the cervical site and in both intraepidermal somatosensory fibers and autonomic fibers surrounding SG, SbG, and MAP. Finally, we tested several Abs against different phosphorylated epitopes of τ by IF (Table 1): Threonine212 (pThr212), Serine262 (pSer262), Serine396 (pSer396), Serine404 (pSer404). However, we did not detect a positive signal in the skin by IF.

Two τ isoforms and phosphorylated τ are present in skin

To analyze τ isoforms expressed in skin lysates at the ankle and cervical sites, samples (10 subjects per HC, PD, PSP/CBD, and 9 for MSA) were tested with Tau and Tau13 antibodies (Table 1, Fig. 3A-B) and compared to human recombinant tau ladder (Sigma-Aldrich, Saint Louis USA, 1:5000). In skin lysate, two major bands were displayed with both antibodies: one at 55kDa, which co-migrated with 0N4R/1N3R isoform, and one at 70kDa corresponding to the 2N4R isoform. Big-tau, the high molecular weight isoform of τ identified in peripheral nerves, was not detected in the skin.

In all groups pThr212, pSer262, and pSer404 Abs detected both bands at 55 kDa and 70 kDa at the ankle and cervical sites (Fig. 3F, G, I), while pSer396 Ab detected mainly the band at 70kDa (Fig. 3H). In all subjects, phosphorylated τ resulted more abundant at the cervical site by semiquantitative analysis of bands intensity (P=0.001), while no significant difference was found between groups. As a negative control, Abs for phosphorylated forms of τ did not mark the un-phosphorylated isoforms of human recombinant τ (Tau ladder, Fig. 3F-I).

2N and 4R mRNAs are more expressed in PSP/CBD

The analysis of the alternative splicing by PCR showed the presence of the 2N variant in skin samples and a lower amount of 1N, while the 0N was never observed. Regarding the splicing at C-terminal, we observed mainly the 4R and, in some cases, a fainter 3R isoform mainly in HC and PD. Therefore, according to PCR results, the main transcript variants were 2N and 4R (Fig. 3C).

The quantification by real-time PCR of *MAPT* gene in skin showed, as expected, a reduced expression compared to the brain and a trend in reduced expression in cervical skin compared to the ankle in PD but no significant difference among and within groups (Fig. 3D). Since we observed mainly the 2N and 4R by PCR assay, we performed the real-time PCR considering primers specific for these isoforms (Fig. 3E-F). The 2N transcript was higher at the cervical than ankle, and while PD and MSA showed similar levels to HC, the PSP/CBD group displayed a major increase of the 2N variant at both anatomical sites compared to the other groups and also

compared to the brain control. The 4R transcript showed a similar level at both anatomical regions and, similarly to 2N, an increase in the PSP/CBD group.

Skin total τ concentration is a biomarker for PSP/CBD diagnosis

The amount of total τ protein was quantified by ELISA assay using Tau Ab, which targets un-phosphorylated and phosphorylated τ at Ser262 τ. Skin lysates from 65 subjects were analyzed (HC=20, PD=26, MSA=9, PSP/CBD=10). Considering the two anatomical sites separately, the PSP/CBD group showed significantly more τ than PD and MSA in cervical skin (Fig. 4A, Supplementary Table 2). No differences were observed between the two anatomical sites within groups (Fig. 4A). A higher amount of τ considering both locations (compound τ) was found in PSP/CBD than in all other groups (Fig. 4A). Univariate logistic regression analysis (Table 3) showed a significant association of compound τ concentration and PSP/CBD diagnosis *vs*. all other groups [OR 1.94 (CI: 1.18-3.18), p=0.008] and *vs*. synucleinopathies (MSA/PD) [OR 2.09 (CI: 1.15-3.82), p=0.01]. This association was still significant after adjusting for age, gender, and LEDD in a multivariate model [OR 7.4 (CI: 1.27-43.950), p=0.02, Table 3].

These results were confirmed by ROC curve analysis; compound τ concentration allowed the identification of PSP/CBD group *vs*. PD (*P*=0.025, AUC=0.812) and *vs*. MSA (*P*=0.004, AUC=0.900), while for PSP/CBD *vs*. HC, the best performance was obtained by τ amount at ankle site (*P*=0.017, AUC=0.774) (Fig. 4B, Supplementary Table 3).

Skin τ concentration and IENFD stratify subjects according to the clinical diagnosis

IENFD was assessed as a measure of small fiber neuropathy and a marker of neurodegeneration. While PD and MSA showed a significant reduction of total and ankle IENFD compared to HC (Table 2), PSP/CBD patients did not present skin denervation compared to HC.

IENFD contributes to the stratification of all groups simultaneously; a linear discriminant analysis model based on τ protein expression and IENFD at both sites allowed the separation of subjects according to their clinical diagnosis with 53.8% accuracy (Fig. 4C, Leave-one-out validation 47.7%). In particular, HC could be separated from patients (PD, MSA, PSP/CBD)

with 73.8% accuracy (Leave-one-out validation 69.2%) and PSP/CBD from synucleinopathies with 82.2% accuracy (Leave-one-out validation 77.8%). Of interest, PSP/CBD were discriminated from PD and MSA with 77.8% and 84.2% accuracy, respectively (Leave-one-out validation 72.2% and 68.4%, respectively).

Skin τ concentration correlates with clinical scales

In HC, compound and cervical τ concentration inversely correlated with age, showing a decrement of the protein with aging (Fig. 5A-B). In MSA, compound concentration directly correlated with COMPASS-31 OH and COMPASS-31 BL, while ankle τ directly correlated with COMPASS-31 OH and cervical τ with COMPASS-31 BL (Fig. 5C-F). In PSP/CBD, compound and ankle τ inversely correlated with MoCa (Fig. 5G-H). No correlations were observed in the PD group.

Discussion

This study demonstrated that τ protein is highly expressed in human epidermal somatosensory nerve fibers and cholinergic/adrenergic nerves surrounding dermal autonomic structures, such as SG, MAP, and SbG. In particular, we demonstrated an increased amount of τ both at transcript and protein levels in skin biopsies of patients with PSP/CBD ~~tauopathies~~ compared to healthy subjects and patients with PD and MSA. This is of relevance because it highlights that accumulation of τ occurs in the peripheral as well as in the central nervous system, and it can be detected in an easily accessible tissue such as skin.

A previous study in abdominal skin biopsy of patients with tauopathies using HT7 antibody against full-length τ, demonstrated τ immunoreactivity only in autonomic fibers surrounding SG[23]. The discrepancy is probably explained by technical issues: formalin-fixed and 4-μm-thick paraffin-embedded sections were used in the previous study, while we used PLP 2% fixative and 50-μm sections. Indeed, formalin fixation reduces the integrity of peripheral antigen retrieval and is not suitable for the study of intraepidermal small nerve fibers[45]. Besides, thicker tissue sections are required for adequate skin nerve fibers sampling since a standard paraffin-embedded tissue section provides only a fraction of the tissue volume obtained with a 20–50-mm frozen

tissue section[46]. In addition, thin tissue sections, by disrupting the nerve fiber structure, reduce the ability to visualize intraneural proteins such as τ[45].

In the skin, by Wb, we detected two bands, at 55kDa and 70 kDa, differently from the human adult brain, which presents six τ isoforms[47]. The 55KDa isoform was also observed in abdominal[24] and cervical skin[26], and in colon mucosa samples[16] and co-migrated with the 0N4R-1N3R isoforms expressed in the adult human brain, similarly to what has been demonstrated for τ in the gastro-enteric system[16]. Indeed, skin and gastro-enteric tissues comprise small nerve fibers encompassing amyelinated somatosensory fibers (epidermis) and thinly myelinated Aδ (dermis and autonomic nervous system), which share anatomical and physiological characteristics with the dopaminergic and cholinergic system, prone respectively to synucleinopathies and tauopathies[17]. The 70kDa band was not previously observed in the skin; however, it was confirmed by a panel of different antibodies, so that it is unlikely unspecific. Consistently with previous evidence[16,24], we did not detect the peripheral τ isoform named "Big-tau" at 110KDa[48] in the skin. Big-tau is generated by the incorporation of exon 4a that doubles the N-terminal domain, and allows a greater stabilization and spacing between the microtubules in large diameter peripheral nerves, such as sciatic nerves and central process projecting to the dorsal horn of the spinal cord[49]. Thus, Big-tau is likely absent in skin innervation where small fibers are predominant.

The transcript analysis of τ revealed the 2N and 4R variants are the most frequent in the skin; we observed mainly the 4R in all groups and the 3R in HC and PD. This is of interest since we know that in PSP and CBD, the abnormal τ aggregates are composed primarily of 4R isoforms and that in neurodegenerative disease, the ratio of 3R/4R is altered[50]. Of note, quantitative analysis of isoform transcripts showed a major increase of 2N and 4R mRNA in the skin of PSP/CBD compared to the other groups and the healthy brain sample. In physiological conditions, the 2N represents only the 10% of τ isoforms in the brain[50] and displays a higher propensity for somatodendritic localization; thus, this increase in the skin axonal compartment looks abnormal[51]. Another study has demonstrated that protein interactors of 2N τ isoforms are highly enriched in disease-related pathways[52]. In line with the increased level of the transcript, we also demonstrated an increased amount of total τ protein in the skin of PSP/CBD, and it is known that the expression level of substrates can amplify the pathogenic seed and contribute to the selected vulnerability of different neuronal populations in misfolded protein-associated neurodegenerative

diseases[53,54]. Further, recent evidence suggests that τ can assemble into fibrils and filaments before post-translational modification, such as phosphorylation and ubiquitination[55]. Beyond confirming the utility of skin biopsy analysis for diagnostic purposes, these results may have relevance in terms of mechanisms of disease in tauopathies.

We demonstrated phosphorylated τ species in the skin in both HC and patients with neurodegenerative disorders by Wb and not by IF, likely due to the lower sensitivity of IF. In all groups, phosphorylated τ was more abundant at the cervical site. The presence of phosphorylated τ in healthy conditions is consistent with an increasing body of evidence suggesting how τ protein can be physiologically regulated by phosphorylation/dephosphorylation processes[4]. Further, phosphorylation at Ser262, Ser396, Ser404 were already demonstrated in non-pathological conditions[4,56]. Moreover, it has been observed that τ protein freshly isolated from surgical brain tissues presents a more highly phosphorylated state than normal adult human τ from autoptic studies due to the intense dephosphorylation activity of the postmortem period and that adult human brain τ is phosphorylated at many of the same sites as Alzheimer's disease paired helical filaments[57]. The finding of phosphorylated τ in synucleinopathies is not unexpected. In a previous work on postmortem PD striatum, it has been shown that τ was hyperphosphorylated at Ser262 among other epitopes[11], and a more recent one showed that τ was hyperphosphorylated at ten epitopes in PD striatum, sharing 50% overlap with Alzheimer's disease[58]. Previous studies showed a greater AT8 (pS202/T205) immunoreactivity in skin biopsies of patients with Alzheimer's disease than HC and with PSP than PD, while no differences were detected with PHF-1 (pSer396/Ser404)[25,26]. We did not find specific pattern of phosphorylation in the skin of PSP/CBD; this is possibly explained by methodological issues, since increased phosphorylated sites are usually detected in insoluble aggregates of τ derived from brain of patients, while we analyzed the soluble fraction only.

We found a significantly higher concentration of τ was measured by ELISA in the skin of PSP/CBD compared to the other groups. Increased τ concentration in skin predicted the PSP/CBD diagnosis after adjusting for age, gender and LEDD, and ROC curve analysis demonstrated an optimal performance, especially at the cervical site, in discriminating PSP/CBD from synucleinopathies, PD, and MSA. This is of clinical relevance as discriminating PSP/CBD *vs*. PD and *vs*. MSA is often a challenging task also for movement disorders experts. Furtherly, τ protein concentration in skin correlated with cognitive impairment in PSP/CBD.

Between the two anatomical sites, cervical skin biopsy showed the largest differences among groups and the highest diagnostic performance. The diagnostic potential of cervical skin biopsy in differentiating PD and AP was also demonstrated by measuring α-Synuclein oligomers by proximity ligation assay[22]. The cervical area possibly bears the advantage of being anatomically closer to the CNS and brainstem and less exposed to confounders such as peripheral neuropathies that are more frequent in the aging population. This data, taken together, push towards a deeper and combined evaluation of τ and α-Synuclein as well as their pathologic forms in cervical skin as a promising diagnostic tool to differentiate misfolding protein-related neurodegenerative disorders. The increased expression of τ in skin biopsy of patients with tauopathies is also relevant because it sheds light on possible pathological events occurring in the peripheral nervous system. In supporting a potential role of τ in causing peripheral neurodegeneration, a recent work showed that overexpressing human non-mutant τ in mice is associated with peripheral neuropathy with somatofugal degeneration[59]. In fact, τ plays an important role in stabilizing neuronal microtubules and regulating axonal transport as well as mitochondria homeostasis[17], and an overexpression/dysfunction may cause axonal degeneration. On the other hand, in this study, we did not find a clear intraepidermal nerve fiber reduction in PSP/CBD, while a small fiber neuropathy was detected in PD and MSA. Thus, it is conceivable that α-Synuclein is associated with a dying-back degeneration while τ may be involved in more centrifugal-like neurotoxicity.

Limitations of this study are the relatively small number of subjects evaluated and the lack of a postmortem pathological confirmation of the clinical diagnosis. Besides, we analyzed only a few of the numerous phosphorylated epitopes of τ, and it would be appropriate to investigate also other post-translation modifications such as acetylation or ubiquitination dysregulation that may have a significant role in pathology[5,6] as well as it would be of interest to analyze insoluble τ aggregates in the skin of PSP/CBD and synucleinopathies. Further, we used a custom ELISA assay, and for reproducibility in future studies, it would be recommended that commercially available ELISA for Tau would be utilized. However, the strengths of the study are the evaluation of a prospective cohort with a group of healthy, age-matched subjects and the exclusion of other concomitant systemic pathologies and possible confounders like dopaminergic treatment.

In conclusion, this comprehensive study accurately characterized the presence of τ protein in skin biopsies of multiple neurodegenerative disorders. It raises new questions about the pathogenesis of tauopathies, but it also shows how skin biopsy is a robust research tool in the field of diagnostic biomarkers for neurodegenerative diseases.

Acknowledgements

The authors are very grateful to all the patients and their relatives who participated in this study. They are grateful to Mrs. Nicole Vago and Mrs. Mara Kuster, CTU nurses, for their valuable work on the clinical database.

Funding

The research leading to these results received funding from FIDINAM 05.2020, Parkinson Schweiz and Jacques und Gloria Gossweiler Stiftung.

Competing interests

The authors report no competing interests.

Supplementary material

'Supplementary material is available at *Brain* online'.

References

1 Andreadis, A. Misregulation of tau alternative splicing in neurodegeneration and dementia. *Prog Mol Subcell Biol* **44**, 89-107, doi:10.1007/978-3-540-34449-0_5 (2006).

2 Martin, L., Latypova, X. & Terro, F. Post-translational modifications of tau protein: implications for Alzheimer's disease. *Neurochem Int* **58**, 458-471, doi:10.1016/j.neuint.2010.12.023 (2011).

3 Morris, M. *et al.* Tau post-translational modifications in wild-type and human amyloid precursor protein transgenic mice. *Nat Neurosci* **18**, 1183-1189, doi:10.1038/nn.4067 (2015).

4 Hanger, D. P., Anderton, B. H. & Noble, W. Tau phosphorylation: the therapeutic challenge for neurodegenerative disease. *Trends Mol Med* **15**, 112-119, doi:10.1016/j.molmed.2009.01.003 (2009).

5 Min, S. W. *et al.* Acetylation of tau inhibits its degradation and contributes to tauopathy. *Neuron* **67**, 953-966, doi:10.1016/j.neuron.2010.08.044 (2010).

6 Petrucelli, L. *et al.* CHIP and Hsp70 regulate tau ubiquitination, degradation and aggregation. *Hum Mol Genet* **13**, 703-714, doi:10.1093/hmg/ddh083 (2004).

7 Alonso, A., Zaidi, T., Novak, M., Grundke-Iqbal, I. & Iqbal, K. Hyperphosphorylation induces self-assembly of tau into tangles of paired helical filaments/straight filaments. *Proc Natl Acad Sci U S A* **98**, 6923-6928, doi:10.1073/pnas.121119298 (2001).

8 Braak, E., Braak, H. & Mandelkow, E. M. A sequence of cytoskeleton changes related to the formation of neurofibrillary tangles and neuropil threads. *Acta Neuropathol* **87**, 554-567, doi:10.1007/bf00293315 (1994).

9 Grundke-Iqbal, I. *et al.* Abnormal phosphorylation of the microtubule-associated protein tau (tau) in Alzheimer cytoskeletal pathology. *Proc Natl Acad Sci U S A* **83**, 4913-4917, doi:10.1073/pnas.83.13.4913 (1986).

10 Kovacs, G. G. Tauopathies. *Handb Clin Neurol* **145**, 355-368, doi:10.1016/B978-0-12-802395-2.00025-0 (2017).

11 Wills, J. *et al.* Elevated tauopathy and alpha-synuclein pathology in postmortem Parkinson's disease brains with and without dementia. *Exp Neurol* **225**, 210-218, doi:10.1016/j.expneurol.2010.06.017 (2010).

12 Rong, Z. *et al.* Phosphorylated alpha-synuclein and phosphorylated tau-protein in sural nerves may contribute to differentiate Parkinson's disease from multiple system atrophy and progressive supranuclear paralysis. *Neuroscience Letters* **756**, doi:ARTN 135964 10.1016/j.neulet.2021.135964 (2021).

13 Nagaishi, M., Yokoo, H. & Nakazato, Y. Tau-positive glial cytoplasmic granules in multiple system atrophy. *Neuropathology* **31**, 299-305, doi:10.1111/j.1440-1789.2010.01159.x (2011).

14 Arnold, S. E. *et al.* Olfactory epithelium amyloid-beta and paired helical filament-tau pathology in Alzheimer disease. *Ann Neurol* **67**, 462-469, doi:10.1002/ana.21910 (2010).

15 Hattori, H. *et al.* The tau protein of oral epithelium increases in Alzheimer's disease. *J Gerontol A Biol Sci Med Sci* **57**, M64-70, doi:10.1093/gerona/57.1.m64 (2002).

16 Lionnet, A. *et al.* Characterisation of tau in the human and rodent enteric nervous system under physiological conditions and in tauopathy. *Acta Neuropathol Commun* **6**, 65, doi:10.1186/s40478-018-0568-3 (2018).

17 Vacchi, E., Kaelin-Lang, A. & Melli, G. Tau and Alpha Synuclein Synergistic Effect in Neurodegenerative Diseases: When the Periphery Is the Core. *Int J Mol Sci* **21**, doi:10.3390/ijms21145030 (2020).
18 Donadio, V. *et al.* Skin nerve alpha-synuclein deposits: a biomarker for idiopathic Parkinson disease. *Neurology* **82**, 1362-1369, doi:10.1212/WNL.0000000000000316 (2014).
19 Doppler, K. *et al.* Distinctive distribution of phospho-alpha-synuclein in dermal nerves in multiple system atrophy. *Mov Disord* **30**, 1688-1692, doi:10.1002/mds.26293 (2015).
20 Melli, G. *et al.* Cervical skin denervation associates with alpha-synuclein aggregates in Parkinson disease. *Ann Clin Transl Neurol* **5**, 1394-1407, doi:10.1002/acn3.669 (2018).
21 Nolano, M. *et al.* Small fiber pathology parallels disease progression in Parkinson disease: a longitudinal study. *Acta Neuropathol* **136**, 501-503, doi:10.1007/s00401-018-1876-1 (2018).
22 Vacchi, E. *et al.* Alpha-synuclein oligomers and small nerve fiber pathology in skin are potential biomarkers of Parkinson's disease. *npj Parkinson's Disease* **7**, 119, doi:10.1038/s41531-021-00262-y (2021).
23 Dugger, B. N. *et al.* Tau immunoreactivity in peripheral tissues of human aging and select tauopathies. *Neurosci Lett* **696**, 132-139, doi:10.1016/j.neulet.2018.12.031 (2019).
24 Dugger, B. N. *et al.* The Presence of Select Tau Species in Human Peripheral Tissues and Their Relation to Alzheimer's Disease. *J Alzheimers Dis* **54**, 1249, doi:10.3233/JAD-169007 (2016).
25 Rodriguez-Leyva, I. *et al.* Parkinson disease and progressive supranuclear palsy: protein expression in skin. *Ann Clin Transl Neurol* **3**, 191-199, doi:10.1002/acn3.285 (2016).
26 Rodriguez-Leyva, I. *et al.* Presence of Phosphorylated Tau Protein in the Skin of Patients with Alzheimer Disease. *Annals of Neurology* **74**, S63-S63 (2013).
27 Hughes, A. J., Daniel, S. E., Kilford, L. & Lees, A. J. Accuracy of clinical diagnosis of idiopathic Parkinson's disease: a clinico-pathological study of 100 cases. *J Neurol Neurosurg Psychiatry* **55**, 181-184, doi:10.1136/jnnp.55.3.181 (1992).
28 Gilman, S. *et al.* Second consensus statement on the diagnosis of multiple system atrophy. *Neurology* **71**, 670-676, doi:10.1212/01.wnl.0000324625.00404.15 (2008).
29 Hoglinger, G. U. *et al.* Clinical diagnosis of progressive supranuclear palsy: The movement disorder society criteria. *Mov Disord* **32**, 853-864, doi:10.1002/mds.26987 (2017).
30 Armstrong, M. J. *et al.* Criteria for the diagnosis of corticobasal degeneration. *Neurology* **80**, 496-503, doi:10.1212/WNL.0b013e31827f0fd1 (2013).
31 Hoehn, M. M. & Yahr, M. D. Parkinsonism: onset, progression and mortality. *Neurology* **17**, 427-442, doi:10.1212/wnl.17.5.427 (1967).
32 Fahn S, E. R., UPDRS program members. Unified Parkinsons Disease Rating Scale. In: Fahn S, Marsden CD, Goldstein M, Calne DB, editors. . Recent developments in Parkinsons disease, vol 2. . *Florham Park, NJ: Macmillan Healthcare Information*, 153-156 (1987).
33 Folstein, M. F., Folstein, S. E. & McHugh, P. R. "Mini-mental state". A practical method for grading the cognitive state of patients for the clinician. *J Psychiatr Res* **12**, 189-198, doi:10.1016/0022-3956(75)90026-6 (1975).

34 Nasreddine, Z. S. *et al.* The Montreal Cognitive Assessment, MoCA: a brief screening tool for mild cognitive impairment. *J Am Geriatr Soc* **53**, 695-699, doi:10.1111/j.1532-5415.2005.53221.x (2005).

35 Beck AT, S. R., Brown GK. BDI-II: Beck Depression Inventory Manual. (1996).

36 Sletten, D. M., Suarez, G. A., Low, P. A., Mandrekar, J. & Singer, W. COMPASS 31: a refined and abbreviated Composite Autonomic Symptom Score. *Mayo Clin Proc* **87**, 1196-1201, doi:10.1016/j.mayocp.2012.10.013 (2012).

37 Stiasny-Kolster, K. *et al.* The REM sleep behavior disorder screening questionnaire - A new diagnostic instrument. *Movement Disord* **22**, 2386-2393, doi:10.1002/mds.21740 (2007).

38 Tomlinson, C. L. *et al.* Systematic Review of Levodopa Dose Equivalency Reporting in Parkinson's Disease. *Movement Disord* **25**, 2649-2653, doi:10.1002/mds.23429 (2010).

39 Vacchi, E., Pinton, S., Kaelin-Lang, A. & Melli, G. Targeting Alpha Synuclein Aggregates in Cutaneous Peripheral Nerve Fibers by Free-floating Immunofluorescence Assay. *J Vis Exp*, doi:10.3791/59558 (2019).

40 Lauria, G. *et al.* EFNS guidelines on the use of skin biopsy in the diagnosis of peripheral neuropathy. *Eur J Neurol* **12**, 747-758, doi:10.1111/j.1468-1331.2005.01260.x (2005).

41 Lauria, G. *et al.* European Federation of Neurological Societies/Peripheral Nerve Society Guideline on the use of skin biopsy in the diagnosis of small fiber neuropathy. Report of a joint task force of the European Federation of Neurological Societies and the Peripheral Nerve Society. *Eur J Neurol* **17**, 903-912, e944-909, doi:10.1111/j.1468-1331.2010.03023.x (2010).

42 Lauria, G., Lombardi, R., Camozzi, F. & Devigili, G. Skin biopsy for the diagnosis of peripheral neuropathy. *Histopathology* **54**, 273-285, doi:10.1111/j.1365-2559.2008.03096.x (2009).

43 Provitera, V. *et al.* A multi-center, multinational age- and gender-adjusted normative dataset for immunofluorescent intraepidermal nerve fiber density at the distal leg. *European Journal of Neurology* **23**, 333-338, doi:10.1111/ene.12842 (2016).

44 Livak, K. J. & Schmittgen, T. D. Analysis of relative gene expression data using real-time quantitative PCR and the 2(-Delta Delta C(T)) Method. *Methods* **25**, 402-408, doi:10.1006/meth.2001.1262 (2001).

45 Gibbons, C. *et al.* Reader Response: In Vivo Distribution of alpha-Synuclein in Multiple Tissues and Biofluids in Parkinson Disease. *Neurology* **96**, 964-965, doi:10.1212/WNL.0000000000011941 (2021).

46 Gibbons, C. H., Garcia, J., Wang, N., Shih, L. C. & Freeman, R. The diagnostic discrimination of cutaneous alpha-synuclein deposition in Parkinson disease. *Neurology* **87**, 505-512, doi:10.1212/WNL.0000000000002919 (2016).

47 Lee, G., Cowan, N. & Kirschner, M. The primary structure and heterogeneity of tau protein from mouse brain. *Science* **239**, 285-288, doi:10.1126/science.3122323 (1988).

48 Goedert, M., Spillantini, M. G. & Crowther, R. A. Cloning of a big tau microtubule-associated protein characteristic of the peripheral nervous system. *Proc Natl Acad Sci U S A* **89**, 1983-1987, doi:10.1073/pnas.89.5.1983 (1992).

49 Fischer, I. & Baas, P. W. Resurrecting the Mysteries of Big Tau. *Trends Neurosci* **43**, 493-504, doi:10.1016/j.tins.2020.04.007 (2020).

50 Limorenko, G. & Lashuel, H. A. Revisiting the grammar of Tau aggregation and pathology formation: how new insights from brain pathology are shaping how we study and target Tauopathies. *Chem Soc Rev* **51**, 513-565, doi:10.1039/d1cs00127b (2022).
51 Bachmann, S., Bell, M., Klimek, J. & Zempel, H. Differential Effects of the Six Human TAU Isoforms: Somatic Retention of 2N-TAU and Increased Microtubule Number Induced by 4R-TAU. *Front Neurosci* **15**, 643115, doi:10.3389/fnins.2021.643115 (2021).
52 Liu, C., Song, X., Nisbet, R. & Gotz, J. Co-immunoprecipitation with Tau Isoform-specific Antibodies Reveals Distinct Protein Interactions and Highlights a Putative Role for 2N Tau in Disease. *J Biol Chem* **291**, 8173-8188, doi:10.1074/jbc.M115.641902 (2016).
53 Peng, C., Trojanowski, J. Q. & Lee, V. M. Protein transmission in neurodegenerative disease. *Nat Rev Neurol* **16**, 199-212, doi:10.1038/s41582-020-0333-7 (2020).
54 Luna, E. *et al.* Differential alpha-synuclein expression contributes to selective vulnerability of hippocampal neuron subpopulations to fibril-induced toxicity. *Acta Neuropathol* **135**, 855-875, doi:10.1007/s00401-018-1829-8 (2018).
55 Hasegawa, M. Structure of NFT: Biochemical Approach. *Adv Exp Med Biol* **1184**, 23-34, doi:10.1007/978-981-32-9358-8_2 (2019).
56 Matsuo, E. S. *et al.* Biopsy-derived adult human brain tau is phosphorylated at many of the same sites as Alzheimer's disease paired helical filament tau. *Neuron* **13**, 989-1002, doi:10.1016/0896-6273(94)90264-x (1994).
57 Beharry, C. *et al.* Tau-induced neurodegeneration: mechanisms and targets. *Neurosci Bull* **30**, 346-358, doi:10.1007/s12264-013-1414-z (2014).
58 Duka, V. *et al.* Identification of the sites of tau hyperphosphorylation and activation of tau kinases in synucleinopathies and Alzheimer's diseases. *PLoS One* **8**, e75025, doi:10.1371/journal.pone.0075025 (2013).
59 Marquez, A. *et al.* Tau associated peripheral and central neurodegeneration: Identification of an early imaging marker for tauopathy. *Neurobiol Dis* **151**, 105273, doi:10.1016/j.nbd.2021.105273 (2021).

Figure legends

Figure 1 τ protein in healthy skin. (**A**) Schematic representation of τ protein four domains and binding sites of Abs used for IF. (**B**) Confocal microscopy images of skin sections from HC stained with axonal markers in red (PGP9.5 and βTubIII) and full-length τ markers in green (Tau13, HT7, Tau5, and Tau). For each antibody is shown the staining at the epidermis and dermis, sweat gland (SG), sebaceous gland (SbG), and muscle arrector pili (MAP). On the right, enlargement of intraepidermal small fibers (1) and autonomic fibers in SG (2), SbG (3), and MAP (4) showing in yellow the colocalization between Tau (green) and βTubIII (red). (**C**) IF of skin biopsy from HC showing cholinergic (VIP) and adrenergic innervation (TH) in red and Tau (unphosphorylated and phosphorylated at Ser262 human Tau), in green) in SG (5) and SbG (6). On the right, enlargement showing in yellow the colocalization between Tau (green) and VIP (red, top) and TH (red, bottom). Magnification 40x, scale bar 50μm. Images are representative of at least three independent experiments on 8 subjects.

Figure 2 τ protein in skin in pathological groups. Confocal microscopy images of skin sections from patients with PD, MSA, and PSP/CBD at the ankle and cervical sites. In green unphosphorylated and phosphorylated at Ser262 human Tau and in red βTubIII staining. For each group, images of epidermis and dermis, sweat gland (SG), sebaceous gland (SbG), and muscle arrector pili (MAP) are shown. Magnification 40x, scale bar 50μm. Images are representative of at least three independent experiments in 18 subjects (PD=10, MSA=3, PSP/CBD=5).

Figure 3 Skin τ isoforms and phosphorylated τ. (**A**) Schematic representation of τ isoforms obtained by alternative splicing of exons 2, 3, and 10 (in green) and 4a (purple) in the human nervous system. (**B**) Representative image of Wb analysis of skin lysates from HC, PD, MSA, and PSP/CBD subjects at the ankle and cervical sites, stained with unphosphorylated and phosphorylated at Ser262 human Tau. Images are representative of at least five independent experiments. (**C**) PCR analysis of skin lysates from ankle and cervical sites. Images are representative of at least five independent experiments. (**D**) Real-time PCR analysis of *MAPT* gene, 2N variant (**E**), and 4R variant (**F**) of skin lysates at ankle and cervical sites in pathological groups compared to the healthy human brain. The amount of RNA was normalized to the expression of the housekeeper *RPL27*. For each group, the mean and SD are reported, and each

point represents an experiment. (**G**) Schematic representation of τ protein four domains and binding sites of Abs for phosphorylated τ. (**H-K**) Representative image of Wb analysis of skin lysates from HC, PD, MSA, and PSP/CBD subjects at the ankle and cervical locations, stained with Abs against phosphorylated τ. MW: molecular weight.

Figure 4 Diagnostic value of skin τ protein concentration. (**A**) Skin τ concentration measured by Elisa assay at both anatomical sites and at each anatomical region in HC and pathologic groups. Kruskal-Wallis analysis is shown, data are expressed as median and interquartile ranges. *P*-values < 0.05 were considered significant (*<0.05, **<0.01). (**B**) ROC curves analysis of τ concentration identifying the best cut-off for each parameter. The referral line is reported in grey. For each comparison, the table provides the asymptotic significance, AUC with 95% CI, sensitivity, and specificity for τ expression at the ankle, cervical, and both sites. *P*-values < 0.05 were considered significant. (**C**) The canonical plot stratifies patients according to the clinical diagnosis. The model was built considering τ concentration and IENFD at the ankle and cervical sites. The plot axes (canonical 1 and canonical 2) were calculated from weighted linear combinations of variables to maximize separation between the four groups. Each subject is represented by a point. HC *vs*. patients: accuracy 73.8%, Leave-one-out validation 69.2%. PSP/CBD *vs*. PD: accuracy 77.8%, Leave-one-out validation 72.2%. PSP/CBD *vs*. MSA accuracy 84.2%, Leave-one-out validation 68.4%.

Figure 5 τ protein concentration and clinical scores correlations. Correlations between τ protein concentration and age in HC (blue) and between τ protein concentration and clinical scales in MSA (orange) and PSP/CBD (green). For each correlation, *P*-value (*P*), Pearson's correlation coefficient (R), regression line (black), and 95% confidence interval (dashed line) are reported.

Table 1 List of antibodies

Name	Type	Dilution			Specificity	Company
		IF	Wb	ELISA		
Primary						
Tau	Rb pAb	1:1000	1:200	1:500	Unphosphorylated and phosphorylated at Ser262 human Tau	Abcam
Tau13	Ms mAb	1:1000	1:500	–	Unphosphorylated human Tau, aa 2-18	Santa Cruz Biotechnology
HT7	Ms mAb	1:1000	–	–	Unphosphorylated human Tau, aa 159-163	ThermoFisher Scientific
Tau5	Ms mAb	1:1000	–	–	Unphosphorylated human Tau, aa 218-225	Abcam
pS404	Rb pAb	1:500	1:500	–	Tau phosphorylated at Ser404	ThermoFisher Scientific
pS262	Rb pAb	1:500	1:500	–	Tau phosphorylated at Ser262	ThermoFisher Scientific
pThr212	Rb pAb	1.500	1:500	–	Tau phosphorylated at Thr212	ThermoFisher Scientific
pSer396	Ms mAb	1.500	1:500	–	Tau phosphorylated at Ser396	ThermoFisher Scientific
PGP9.5	Rb pAb	1:1000	–	–	Axonal marker	Abcam
βTubIII	Ms mAb	1:500	–	–	Axonal marker	Sigma Aldrich
TH	Ms mAb	1:200	–	–	Adrenergic nerve fibers	Millipore
VIP	Rb pAb	1:2000	–	–	Cholinergic nerve fibers	Immunostar
Secondary						
Alexa-Fluor 488	G x Ms	1:400	–	–	AffiniPure Goat Anti-Mouse IgG (H+L)	Jackson ImmunoResearch
Alexa-Fluor 488	G x Rb	1:400	–	–	Highly Cross-Adsorbed Goat anti-Rabbit IgG (H+L)	ThermoFisher Scientific
Alexa-Fluor 594	G x Ms	1:400	–	–	Highly Cross-Adsorbed Goat anti-Mouse IgG (H+L)	ThermoFisher Scientific
Alexa-Fluor 594	G x Rb	1:400	–	–	AffiniPure Goat Anti-Rabbit IgG (H+L)	Jackson ImmunoResearch
IRDye® 680RD	G x Ms	/	1:5000	–	IRDye® 680RD Goat anti-Mouse IgG	LI-COR Biosciences
IRDye® 800CW	G x Rb	/	1:5000	–	IRDye® 800CW Goat anti-Rabbit IgG	LI-COR Biosciences
Anti-Rabbit HRP	G x Rb	/	–	1:5000	Goat anti-Rabbit IgG (H+L)-HRP Conjugate	Bio-Rad

Characteristics of primary and secondary antibodies used in this study: name, type, dilution for IF , Wb and ELISA assay, specificity, and company. Abbreviations: Rb (Rabbit), pAb (polyclonal Antibody), Ms (Mouse), mAb (monoclonal Antibody), G (Goat), HRP (horseradish peroxidase).

1 **Table 2 Demographic data and clinical scores**

	HC [*n*=24]	PD [*n*=31]	MSA [*n*=14]	PSP/CBD [*n*=15]	Overall *P*-value	Pairwise Comparisons					
						PD *vs.* HC	MSA *vs.* HC	PSP/CBD *vs.* HC	PD *vs.* MSA	PSP/CBD *vs.* PD	PSP/CBD *vs.* MSA
Age (years)	62 ± 8	67 ± 12	67 ± 8	75 ± 6	**0.011**	0.090	0.105	**0.000**	0.868	0.094	0.065
Sex (ref. male)	12 (50.0%)	17 (54.8%)	4 (28.6%)	7 (46.7%)	0.433	-	-	-	-	-	-
Disease duration (years)	-	5.0 [3.0–9.0]	5.0 [1.8–7.3]	4.0 [3.0–5.0]	0.305	-	-	-	-	-	-
H&Y	-	2.0 [2.0–3.0]	4.0 [3.0–5.0]	4.0 [3.0–4.0]	**0.000**	-	-	-	**0.000**	**0.000**	0.377
MDS-UPDRS-I	-	4.0 [2.0–6.0]	8.0 [6.5–10.5]	12.0 [6.5–22.0]	**0.006**	-	-	-	**0.016**	**0.011**	0.310
MDS-UPDRS-II	-	6.0 [5.0–9.8]	15.0 [8.5–21.0]	17.0 [13.0–27.5]	**0.005**	-	-	-	**0.050**	**0.002**	0.421
MDS-UPDRS-III	-	17.0 [12.0–23.3]	32.5 [23.0–46.5]	31.5 [22.5–41.5]	**0.000**	-	-	-	**0.003**	**0.000**	0.798
MDS-UPDRS-Total	-	28.5 [20.3–37.8]	53.0 [31.5–67.0]	53.0 [39.3–97.5]	**0.004**	-	-	-	**0.050**	**0.001**	0.792
COMPASS-31 OH	-	0.0 [0.0–16.0]	0.0 [0.0–21.0]	0.0 [0.0–20.0]	0.864	-	-	-	-	-	-
COMPASS-31 VM	-	0.0 [0.0–0.0]	0.0 [0.0–0.0]	0.0 [0.0–0.0]	0.222	-	-	-	-	-	-
COMPASS-31 SM	-	0.0 [0.0–4.2]	2.1 [0.0–4.2]	0.0 [0.0–4.2]	0.434	-	-	-	-	-	-
COMPASS-31 GI	-	0.9 [0.0–6.3]	3.7 [0.0–5.8]	0.0 [0.0–6.3]	0.697	-	-	-	-	-	-
COMPASS-31 BL	-	0.0 [0.0–0.0]	0.5 [0.0–2.5]	0.0 [0.0–0.0]	**0.003**	-	-	-	**0.002**	0.795	0.050
COMPASS-31 PM	-	0.0 [0.0–0.0]	0.0 [0.0–0.0]	0.0 [0.0–0.0]	1.000	-	-	-	-	-	-
COMPASS-31 Total	-	6.3 [0.8–24.1]	12.3 [5.5–27.5]	11.9 [4.2–28.0]	0.675	-	-	-	-	-	-
BDI-II	-	6.0 [3.0–8.5]	8.5 [3.7–13.0]	14.0 [8.0–18.0]	**0.006**	-	-	-	0.238	**0.001**	0.068
MMSE	-	30.0 [29.0–30.0]	28.0 [25.5–29.0]	26.0 [22.5–28.0]	**0.000**	-	-	-	**0.004**	**0.000**	0.081
MoCA	-	27.0 [24.0–29.0]	26.0 [21.5–27.7]	20.0 [17.0–24.0]	**0.001**	-	-	-	0.227	**0.000**	**0.011**
Olfactory test	-	7.0 [5.0–9.0]	9.0 [9.0–10.8]	7.0 [4.3–9.8]	0.067	-	-	-	-	-	-
RBD questionnaire	-	3.0 [1.0–5.3]	3.5 [1.0–5.2]	2.5 [0.0–5.0]	0.643	-	-	-	-	-	-
LEDD (mg)	-	495.5 [288.0–775.0]	437.5 [174.8–500.0]	250.0 [100.0–451.0]	0.167	-	-	-	-	-	-
IENFD total (Fibers/mm)	14.9 [11.5–	10.9 [7.3–	11.8 [8.4–	13.5 [7.8–17.3]	**0.044**	**0.014**	**0.013**	0.214	0.985	0.475	0.497

	16.6]	14.8]	13.8]								
IENFD cervical (Fibers/mm)	20.6 [14.7–24.8]	14.3 [10.8–21.5]	18.1 [11.4–21.4]	19.9 [12.4–24.8]	0.288	-	-	-	-	-	-
IENFD ankle (Fibers/mm)	9.1 [7.5–10.6]	5.7 [4.1–9.7]	6.2 [2.9–8.1]	6.7 [4.0–9.7]	**0.029**	**0.012**	**0.010**	0.082	0.781	0.741	0.604

Clinical characteristics of patients. Variables are reported as mean ± SD, median [interquartile range], absolute number (percentage), as appropriate. A P<0.05 was considered significant and shown in bold.

Table 3 τ concentration and likelihood of tauopathies diagnosis

		Univariate		**Multivariate**	
		OR (95% CI)	***P*-value**	**OR (95% CI)**	***P*-value**
PSP/CBD *vs.* PD/MSA	Compound τ	2.09 (1.15–3.82)	**0.015**	7.49 (1.27–43.95)	**0.025**
	Age	1.09 (0.99–1.20)	**0.050**	-	0.111
	Sex	-	0.525	-	0.057
	LEDD	-	0.090	-	0.481

Univariate and multivariate logistic regression analyses were performed to assess the odds ratio (OR) and 95% confidence intervals (95% CI) for τ protein at both sites (compound), Age, Sex, and LEDD, between PSP/CBD group and PD/MSA. An OR greater than 1 indicates an increased likelihood of PSP/CBD diagnosis; P-values < 0.05 were considered significant and shown in bold.

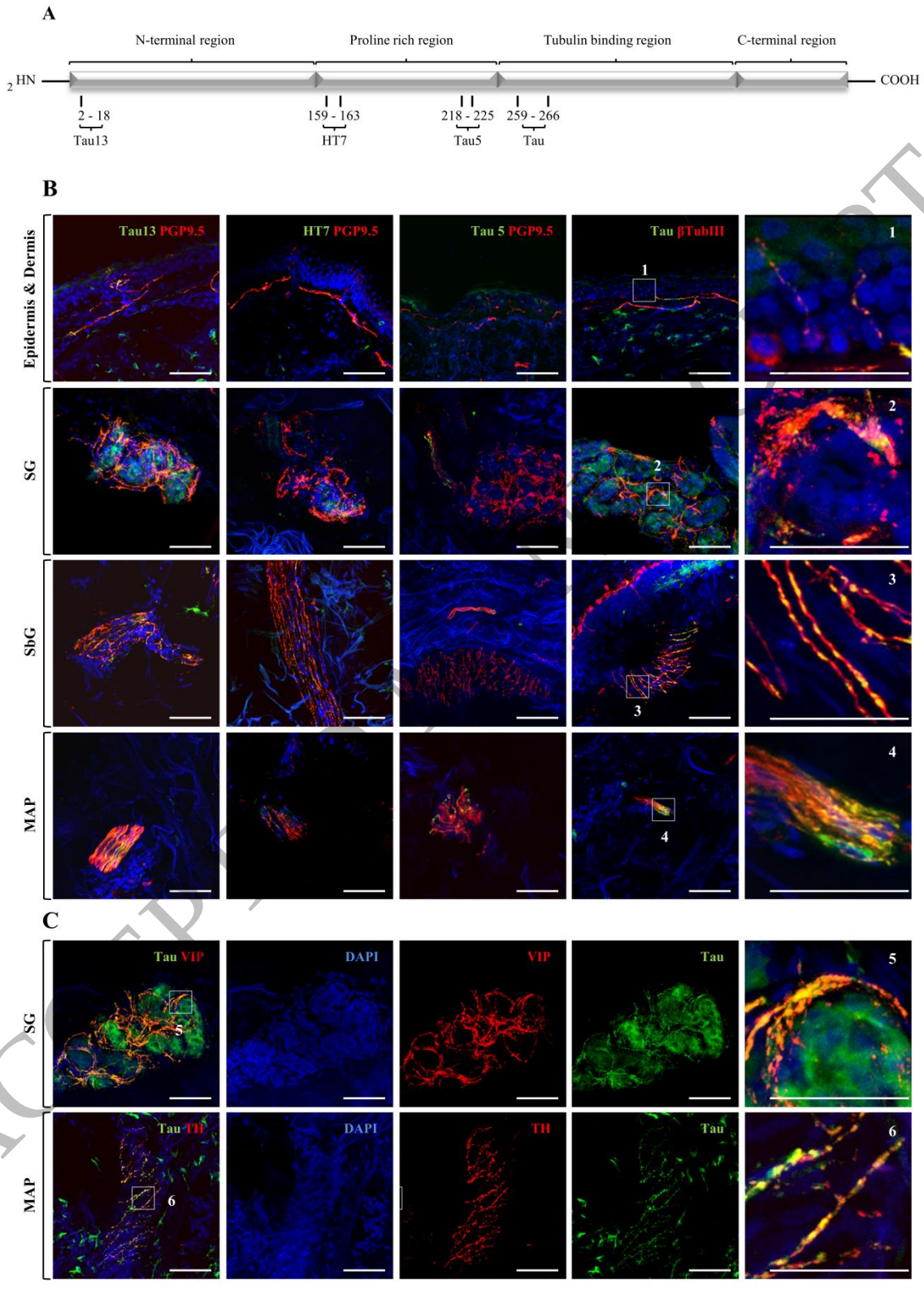

Figure 1
174x234 mm (.09 x DPI)

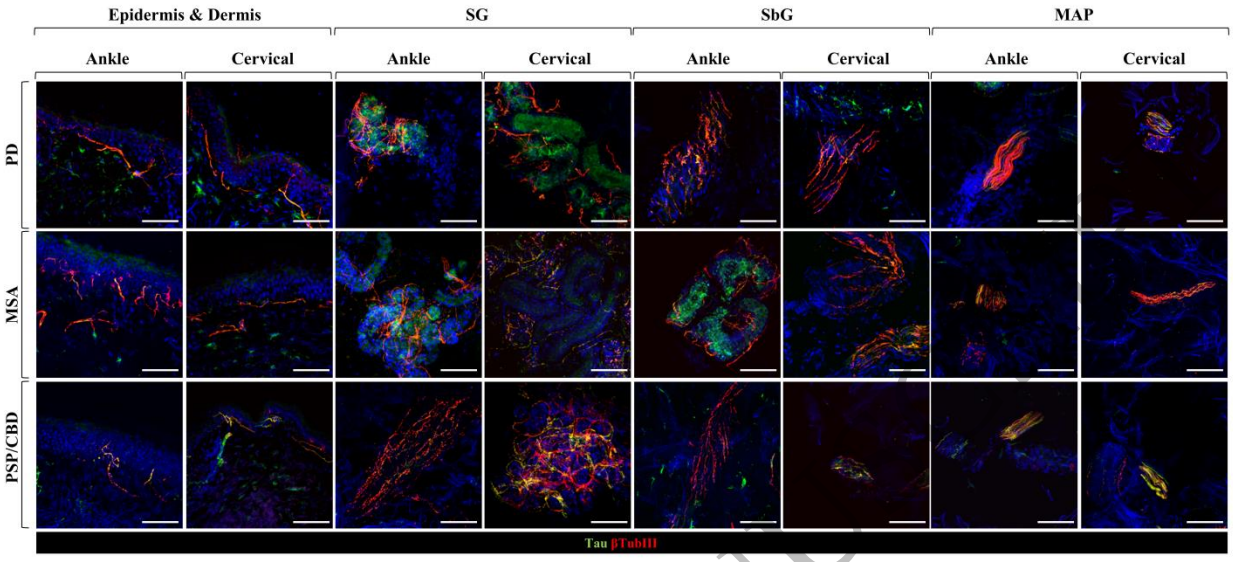

Figure 2
230x170 mm (.09 x DPI)

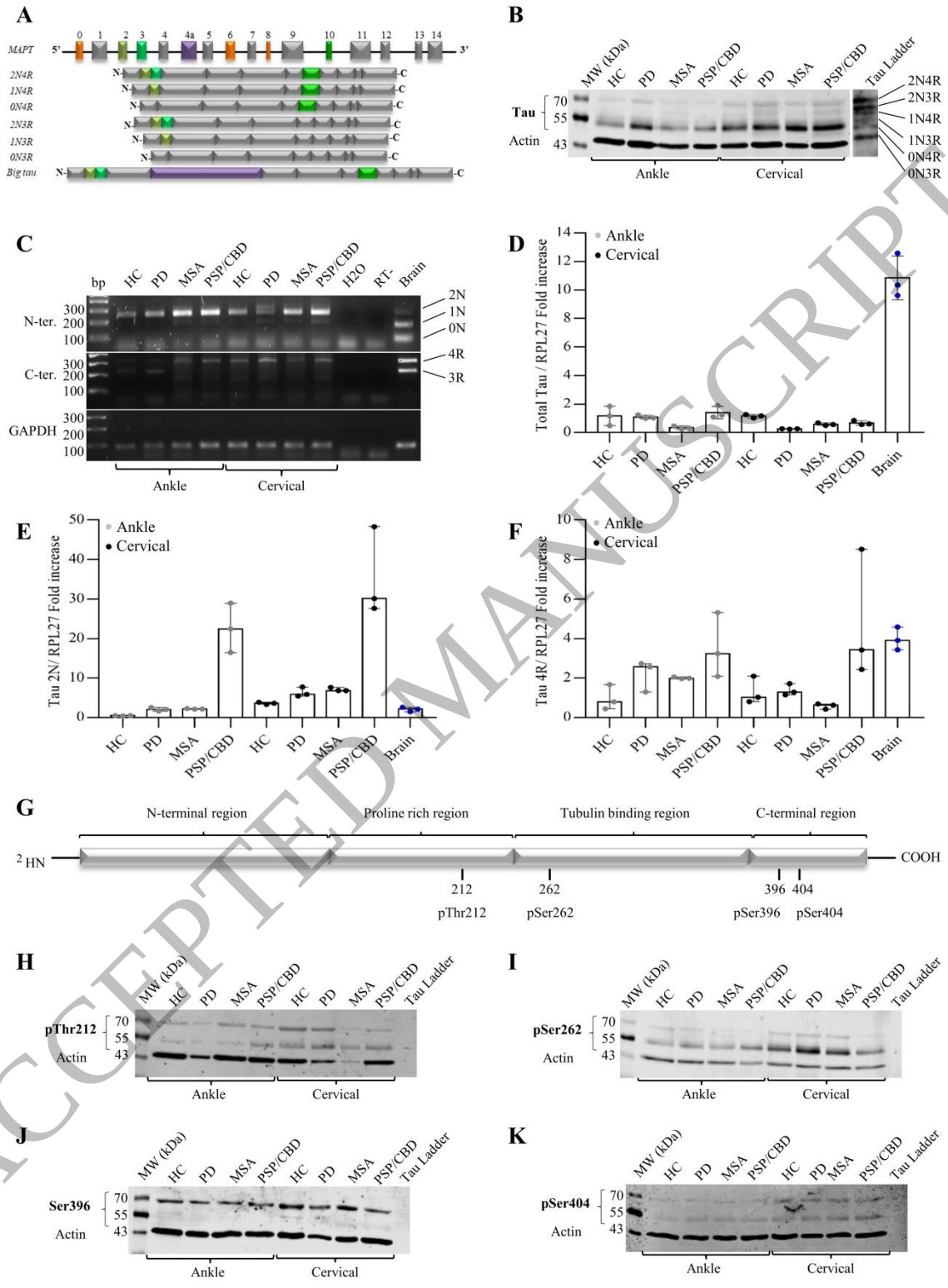

Figure 3
174x234 mm (.09 x DPI)

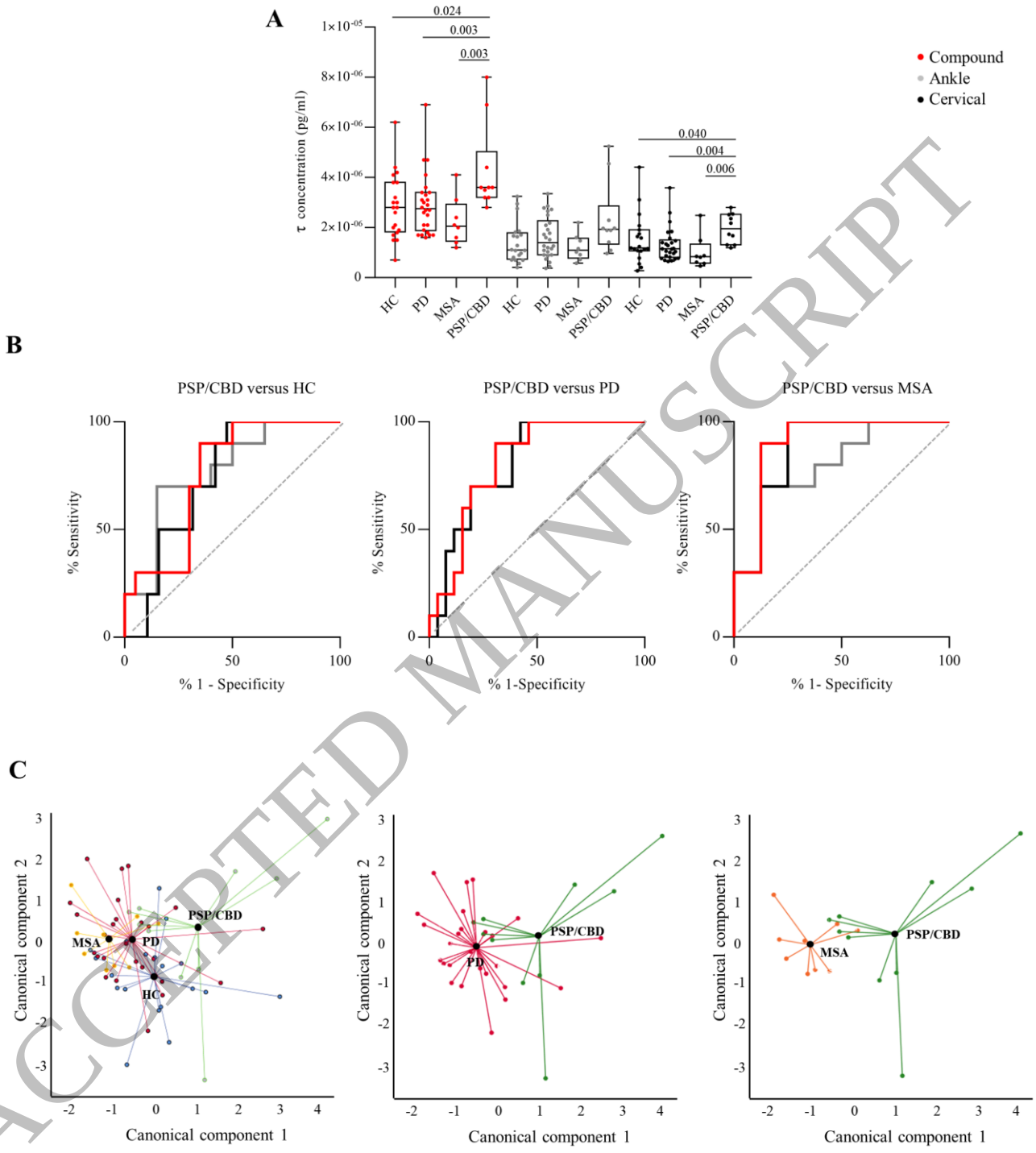

Figure 4
174x194 mm (.09 x DPI)

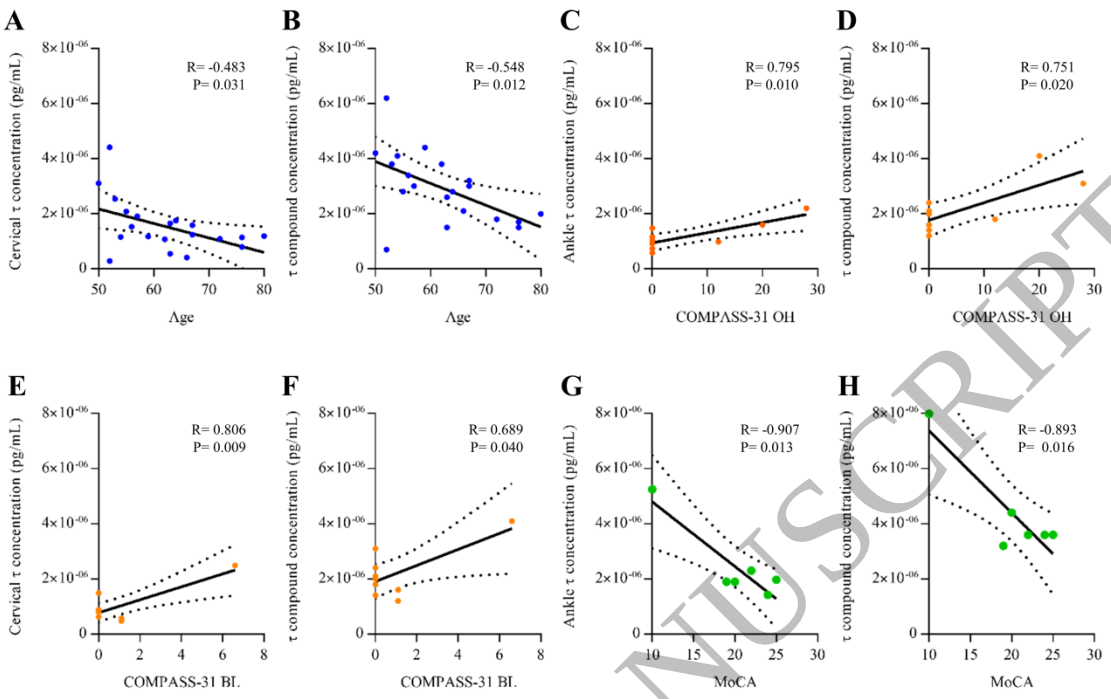

Figure 5
174x234 mm (.09 x DPI)